Cellular/Molecular

Inositol 1,4,5-Trisphosphate 3-Kinase A Functions As a Scaffold for Synaptic Rac Signaling

Il Hwan Kim,[1] Soon Kwon Park,[3] Soon Taek Hong,[1] Yong Sang Jo,[2] Eun Joo Kim,[2] Eun Hye Park,[2] Seung Baek Han,[1] Hee-Sup Shin,[4] Woong Sun,[1] Hyun Taek Kim,[2] Scott H. Soderling,[5,6] and Hyun Kim[1]

[1]Department of Anatomy, College of Medicine, Korea University, Brain Korea 21, Seoul 136-705, Korea, [2]Department of Psychology, Korea University, Seoul 136-701, Korea, [3]School of Alternative Medicine and Health Science, Jeonju University, Jeonju 520-759, Korea, [4]Center for Neural Science, Korea Institute of Science and Technology, Seoul 136-791, Korea, and Departments of [5]Cell Biology and [6]Neurobiology, Duke University Medical School, Durham, North Carolina 27710

Activity-dependent alterations of synaptic contacts are crucial for synaptic plasticity. The formation of new dendritic spines and synapses is known to require actin cytoskeletal reorganization specifically during neural activation phases. Yet the site-specific and time-dependent mechanisms modulating actin dynamics in mature neurons are not well understood. In this study, we show that actin dynamics in spines is regulated by a Rac anchoring and targeting function of inositol 1,4,5-trisphosphate 3-kinase A (IP_3K-A), independent of its kinase activity. On neural activation, IP_3K-A bound directly to activated Rac1 and recruited it to the actin cytoskeleton in the postsynaptic area. This focal targeting of activated Rac1 induced spine formation through actin dynamics downstream of Rac signaling. Consistent with the scaffolding role of IP_3K-A, IP_3K-A knock-out mice exhibited defects in accumulation of PAK1 by long-term potentiation-inducing stimulation. This deficiency resulted in a reduction in the reorganization of actin cytoskeletal structures in the synaptic area of dentate gyrus. Moreover, IP_3K-A knock-out mice showed deficits of synaptic plasticity in perforant path and in hippocampal-dependent memory performances. These data support a novel model in which IP_3K-A is critical for the spatial and temporal regulation of spine actin remodeling, synaptic plasticity, and learning and memory via an activity-dependent Rac scaffolding mechanism.

Introduction

Memory formation and storage in the brain is believed to be mediated by changes in synaptic efficacy and strength (Bliss et al., 2003; Segal, 2005). Dendritic spines, the postsynaptic part of synapses, display a highly dynamic morphology in the developing (Dailey and Smith, 1996) and the mature brain (Yuste and Bonhoeffer, 2001). Because the number and morphology of dendritic spines are linked to synaptic efficacy and neuronal plasticity (Engert and Bonhoeffer, 1999; Maletic-Savatic et al., 1999; Kim et al., 2002; Leuner et al., 2003), mechanisms that modulate the formation and differentiation of spines are thought to be essential for learning and memory (Kennedy et al., 2005). Additionally, abnormal spine morphology has been observed in brain tissue samples of patients with mental retardation (Purpura, 1974).

Filamentous actin (F-actin) is highly enriched in dendritic spines (Matus et al., 1982) and the regulation of actin dynamics plays an essential role in the molecular processes underlying spine morphogenesis (Bonhoeffer and Yuste, 2002; Star et al., 2002) and plasticity (Fukazawa et al., 2003; Penzes et al., 2003; Lin et al., 2005). The key regulators of actin remodeling in postsynaptic spines are the small GTPase proteins such as Rho-A, Cdc42, and Rac1 (Luo, 2002). In particular, Rac1 has been shown to regulate the morphogenesis of dendritic spines by affecting actin dynamics (Nakayama et al., 2000; Tashiro et al., 2000). The activation of Rac1 requires guanine nucleotide exchange factors (GEFs) such as Tiam1 and kalirin (Penzes et al., 2001, 2003; Tolias et al., 2005). However, whether there are mechanisms that are responsible for activity-dependent positioning of activated Rac1 to the dendritic actin cytoskeleton, remains unclear.

Inositol 1,4,5-trisphosphate 3-kinase A (IP_3K-A) is a brain- and neuron-specific molecule that is enriched in dendritic spines (Mailleux et al., 1991). Previously, the only known activity of IP_3K-A was its ability to convert inositol 1,4,5-trisphosphate (IP_3) to inositol 1,3,4,5-tetrakisphosphate (IP_4), thereby reducing the influx of calcium released from endoplasmic reticulum via IP_3 receptor signaling (Irvine et al., 1986; Choi et al., 1990). In addition to its catalytic domain, IP_3K-A also has an F-actin-binding domain of unknown significance in its N terminus (Schell et al., 2001). Because IP_3K-A is enriched in dendritic spines, it has been speculated that IP_3K-A is involved in spine remodeling through its kinase function (Schell and Irvine, 2006). Furthermore, we recently reported that IP_3K-A mRNA and protein are upregulated in rat brain after spatial learning tasks (Kim et al., 2004). Therefore, IP_3K-A appears to be a strong candidate to be involved in the synaptic plasticity underlying learning and

Received May 28, 2009; revised Sept. 19, 2009; accepted Sept. 22, 2009.

This work was supported by Korea Science and Engineering Foundation Grants M103KV010023-07K2201-02310 and M1050000004905J000004900 (H.K.); Korea Health 21 R&D Project, Ministry of Health and Welfare, Republic of Korea Grant 02-PJ1-PG1-CH06-0001 (H.K.); and National Institutes of Health Grant R01-NS059957 (S.H.S.). We are grateful to Drs. Menahem Segal, William C. Wetsel, and Michael D. Ehlers for critical reading of this manuscript, to Drs. Im Joo Rhyu, Byung-Il Choi, Eunjoon Kim, and Dong Ki Kim for advice and consultations throughout this study, to Dr. Ryuichi Shigemoto for providing a GluR1 antibody, and to Mi-Ra Noh and Jee-Woong Kim for technical support.

Correspondence should be addressed to Dr. Hyun Kim, Department of Anatomy, College of Medicine, Korea University, Seoul 136-705, Korea. E-mail: kimhyun@korea.ac.kr.

DOI:10.1523/JNEUROSCI.2483-09.2009

 0270-6474/09/2914039-11$15.00/0

memory. Previous analysis of IP_3K-A knock-out (KO) mice demonstrated the loss of IP_3K-A does not affect intracellular calcium levels in neurons (Jun et al., 1998). Thus, whether or not IP_3K-A plays a functional role via its catalytic activity to modulate synaptic signaling has been an open question. It is possible IP_3K-A may have other, as of yet unexplored, neurophysiological properties that are independent of IP_4 levels.

In the present study, we demonstrate that IP_3K-A promotes structural remodeling of dendritic spines by affecting actin dynamics. Surprisingly, these effects were not induced by the kinase activity of IP_3K-A, but rather by IP_3K-A-mediated targeting of activated Rac1 to the actin cytoskeleton of dendrites. Most importantly, this process occurred during neural activation. We observed that IP_3K-A directly interacts with activated Rac1 and recruits it to the actin cytoskeleton in the spine-rich region after long-term potentiation (LTP) induction. This IP_3K-A scaffolding function supports the local induction of Rac downstream events such as p21-activated kinase (PAK) phosphorylation and dendritic spine formation. Furthermore, IP_3K-A knock-out mice exhibited defects in synaptic plasticity in the dentate gyrus and hippocampal-dependent memory formation. Together, these data suggest a novel kinase-independent role for IP_3K-A as an activity-dependent Rac scaffolding protein in dendritic spine remodeling and memory formation.

Materials and Methods

Animals. Male Sprague Dawley rats (Orient) and mice were housed in a temperature (22°C)-, humidity (50%)-, and light-controlled vivarium (light on at 7:00 P.M./light off at 7:00 A.M.) with *ad libitum* access to food and water. The genetic background of mice was 129Sv × C57BL/6. They were backcrossed >10 times with C57BL/6. We used only littermate mice from heterozygous parents. Animals were treated in accordance with the National Institutes of Health *Guide for the Care and Use of Laboratory Animals*, and formal approval to conduct this experiment was obtained from the animal subjects review board of Korea University.

In vivo *LTP. In vivo* LTP induction using rats was performed essentially as described previously (Fukazawa et al., 2003) with some modifications. Rats were anesthetized with sodium pentobarbital (60 mg/kg) injected intraperitoneally. A concentric electrode was positioned in the region of the perforant path (7.5 mm posterior and 4.0 mm lateral to the bregma). A recording electrode made of tungsten (125 μm in diameter; impedance, 1–6 MΩ; A-M Systems) was positioned ipsilaterally in the dentate gyrus (DG) granule cellular layer (3.8 mm posterior and 2.0 mm lateral to the bregma). For the baseline field potential recording, 50% of the maximum slope was used. To induce LTP, the biphasic square wave form of strong tetanic stimulation (four trains with 15 min intertrain intervals, with each train consisting of 20 bursts of 30 pulses at 400 Hz, delivered at 5 s interburst intervals) was applied to the perforant path. These evoked potentials were amplified (1000×), filtered at 0.1 Hz to 10 kHz bandwidth, and digitized at 10 kHz. Ten minutes after the last tetanus, potentiation was monitored for 45 min.

Cell culture. The rat hippocampus (embryonic, 18.5 d) was dissected and digested with 0.25% trypsin-EDTA (Invitrogen) and trituration. The dissociated cells were plated on poly-D-lysine (Sigma-Aldrich) (50 μg/ml)-precoated coverslips at a density of 7×10^4 cells per 24-well plate. The complete growth medium consisted of Neurobasal medium (Invitrogen) containing B27 supplement (Invitrogen), 0.5 mM L-glutamine (Invitrogen), 25 mM glutamic acid (Sigma-Aldrich), and antibiotics. The neurons were treated with 1 μM AraC (Sigma-Aldrich) to reduce the growth of contaminating non-neuronal cells. HeLa cells were seeded at a density of 2×10^4 cells per 24-well plate and maintained in DMEM (Invitrogen) plus 10% fetal bovine serum (Invitrogen) and antibiotics.

Preparation of constructs. To construct pEGFP-tagged wild-type (WT) and deletion and point mutants of IP_3K-A (GenBank accession number NM_031045), inserts were created by PCR amplification of rat brain cDNA with the appropriate primers (supplemental table, available at www.jneurosci.org as supplemental material), digested with BamHI and HindIII (Promega), and then ligated into pEGFP-C1 vector (Clontech) with T4 DNA ligase (Promega). The GFP-IP_3K-A-K262A was generated by site-directed mutagenesis using the QuikChange II XL mutagenesis kit (Stratagene) with the appropriate primers (Togashi et al., 1997) (supplemental table, available at www.jneurosci.org as supplemental material). To construct DsRed-tagged Rac1 (GenBank accession number NM_134366) and Cdc42/Rac interactive binding (CRIB) (GenBank accession number NM_002576), inserts were created by PCR amplification of rat brain cDNA and AGS cell cDNA, respectively, with appropriate primers (supplemental table, available at www.jneurosci.org as supplemental material). The inserts were digested with EcoRI and BamHI (Promega) and ligated into pDsRed2-C1 vector (Clontech). Next, each construct was transformed into *Escherichia coli* DH5α. For glutathione *S*-transferase (GST)-tagged constructs, inserts were created by PCR amplification of rat brain cDNA with the appropriate primers (supplemental table, available at www.jneurosci.org as supplemental material), and then amplified inserts were digested with BamHI and EcoRI (Promega) and ligated into pGEX-5X-1 vector (pGEX-2TK vector for GST-CRIB) (GE Healthcare), followed by transformation into *E. coli* BL-21 (CodonPlus; Stratagene).

Adenoviral infection and transfection. Adenoviruses (synthesized at Neurogenex) at a concentration of 200 multiplicities of infection were used. For both neurons and HeLa cells, a one-half volume of medium was removed and replaced by virus-containing medium, and the cells returned to the incubator. Transfections of plasmids or small interfering RNA (siRNA) into primary hippocampal neurons were performed in 24-well plates using the calcium phosphate method. Transfections of plasmids or siRNA into HeLa cells are performed using Lipofectamine 2000 (Invitrogen) according to the manufacturer's instructions. After expression, neurons or HeLa cells were fixed with 4% paraformaldehyde, followed by additional experiments.

Statistical analyses. For analysis of a difference between two groups, Student's *t* test or paired *t* test (SPSS 12.0K) was used. When comparing among more than two groups, one-way ANOVA (SPSS 12.0K) was used. ANOVA with repeated measures was used to analyze data from the object recognition and radial arm maze tests (SAS). Scheffé's test, Tukey's test, and Bonfferoni's correction were used for *post hoc* test (SPSS 12.0K). All values were expressed as mean ± SEM, and results were considered statistically significant if $p < 0.05$.

The experimental procedures of *In vivo* LTP for mice, Chemical LTP, GST pulldown assay, Immunoprecipitation, Western blotting, Immunohistochemistry, Immunocytochemistry, siRNA, Electroporation, Protein expression, Subcellular fractionation, Purification of Rac1 protein, Rac1 activity assay, Golgi staining, Object recognition test, and Radial arm maze test can be found in supplemental Experimental Procedures (available at www.jneurosci.org as supplemental material).

Results

IP_3K-A accumulates in dendritic spines on LTP induction

Previously, we reported that learning enhances IP_3K-A protein expression in the hippocampal formation (Kim et al., 2004). The molecular mechanisms underlying this effect were further analyzed *in vivo* and *in vitro*. After induction of LTP in the DG perforant path *in vivo*, we observed a marked accumulation of IP_3K-A immunoreactivity (IR) in the middle and outer molecular layers of DG, which is the synaptic contact region with the medial and lateral perforant path from the entorhinal area (Fig. 1*A*). Densitometric analysis for IP_3K-A IR in DG showed significant increase of density ratio (middle molecular layer/inner molecular layer) in the LTP-induced hemisphere compared with the nontreated contralateral side ($t = 11.09$; $df = 6$; $p < 0.0001$).

For a more detailed examination of individual neurons, LTP was chemically induced in 22 d in vitro (DIV 22) hippocampal primary neurons, and IP_3K-A IR was quantified. Thirty minutes after chemical LTP (c-LTP) induction, the number of spines was

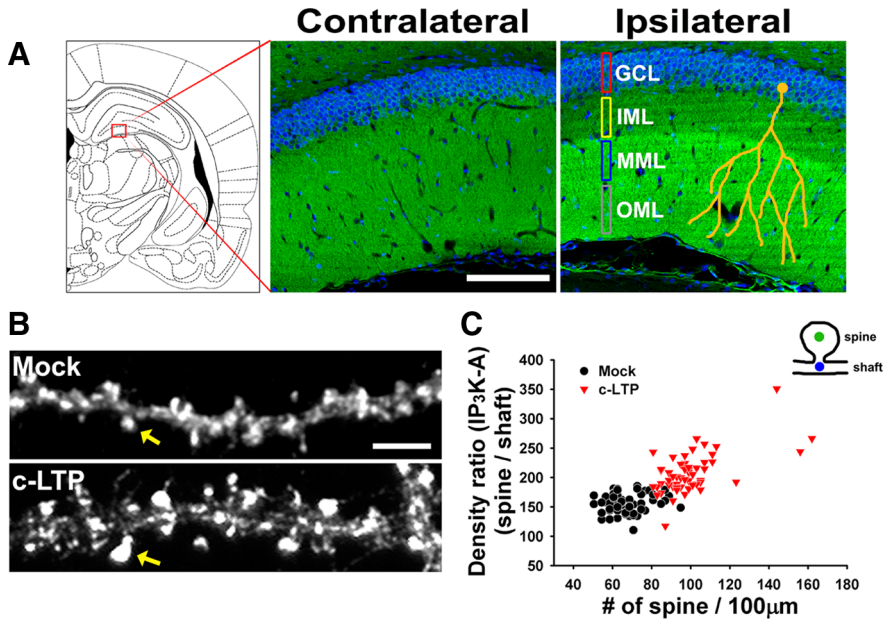

Figure 1. IP_3K-A accumulates in dendritic spines on LTP induction. ***A***, Redistribution of IP_3K-A in DG after *in vivo* LTP induction. One hour after the last tetanus in the perforant path, IP_3K-A IR was observed by immunohistochemistry (green signal). Note the accumulation of IP_3K-A IR in the spine-rich field of DG (MML and OML) only in the LTP-induced hemisphere (ipsilateral). The orange lines represent schematic illustration of a granule cell in DG. Blue signals, Nucleus. GCL, Granule cell layer; IML, inner molecular layer; MML, middle molecular layer; OML, outer molecular layer. Scale bar, 200 μm. ***B***, Immunocytochemical assays showed an increase in density of dendritic spines after c-LTP induction. In c-LTP-treated neurons, endogenous IP_3K-A was densely localized in spines by c-LTP induction (yellow arrows). Scale bar, 3 μm. ***C***, Spine number was correlated with the mean value of the density ratio between dendritic spine and shaft ($r = 0.726$; $p < 0.0001$). Densitometry analysis revealed that neurons with a greater number of spines had more IP_3K-A accumulated in those spines. The schematic figure indicates the calculating points for IP_3K-A density in dendritic spine (green circle, spine; blue circle, shaft).

increased (Fig. 1*B*; supplemental Movie S1, available at www.jneurosci.org as supplemental material) and high levels of GluR1 signals were observed on the spines (supplemental Fig. S1, available at www.jneurosci.org as supplemental material), which is consistent with previous reports (Xie et al., 2005). Interestingly, neurons with a greater number of spines displayed a stronger IP_3K-A IR signal in those spines (Fig. 1*B*). A strong correlation ($r = 0.726$; $p < 0.0001$) existed between spine number and mean value of the density ratio of IP_3K-A (spine/shaft) (Fig. 1*C*). These data suggest dynamic targeting of IP_3K-A to the spine area by neural activation and a possible involvement of IP_3K-A in activity-dependent spine formation.

IP_3K-A promotes dendritic spine formation

To investigate the function of IP_3K-A, we introduced siRNA specific for IP_3K-A into neurons [the specificity of the IP_3K-A siRNA is shown in supplemental Fig. S2 (available at www.jneurosci.org as supplemental material)]. After transfection of IP_3K-A siRNA in combination with green fluorescent protein (GFP)-expressing vectors into DIV 22 hippocampal neurons, GFP^+ neurons exhibited markedly reduced IP_3K-A expression (Fig. 2*A*). Quantification revealed that the density of dendritic spines was also greatly reduced in IP_3K-A siRNA-transfected/GFP^+ neurons when compared with control siRNA-transfected/GFP^+ neurons ($t = 14.17$; df = 52; $p < 0.0001$). To avoid off-target effects of siRNA, we also did rescue experiments and found that the effect of IP_3K-A siRNA on spine formation could be rescued by expression of an siRNA-resistant N-terminal fragment of GFP-IP_3K-A (supplemental Fig. S2, available at www.jneurosci.org as supplemental material). These data indicate that IP_3K-A is required for the development or maintenance of dendritic spines.

To further address the role of IP_3K-A in spontaneous spine formation, IP_3K-A was overexpressed in DIV 22 hippocampal neurons by infection with adenovirus containing full-length IP_3K-A. Eighteen hours after infection, the neurons exhibited a markedly increased number of dendritic structures, and overexpressed GFP-IP_3K-A signals were highly localized in the heads of dendritic protrusions (Fig. 2*B*,*C*). Quantification revealed that the number of protrusions in IP_3K-A-expressing neurons was significantly increased compared with that of the control GFP-infected group ($F_{(3,201)} = 90.03$; Tukey's test, $p < 0.05$) (Fig. 2*G*). Thus, IP_3K-A appears to be able to induce production of new dendritic protrusions.

IP_3K-A catalytic activity regulates calcium levels by modulating the metabolism of IP_3. Yet previous work suggests IP_3K-A may not function to regulate calcium flux in neurons (Jun et al., 1998). Thus, it is important to evaluate whether the function of IP_3K-A in protrusion formation is mediated by its kinase activity. To address this issue, we overexpressed a mutant IP_3K-A containing a point mutation (IP_3K-A-K262A) that lacks kinase activity (Togashi et al., 1997). Remarkably, GFP-IP_3K-A-K262A overexpression produced results similar to those for wild-type IP_3K-A overexpression (Tukey's test, $p < 0.05$) (Fig. 2*E*,*G*). This finding suggested that some function other than the kinase activity of IP_3K-A is essential for the spinogenic activity observed. Consistent with this, deletion of the actin-binding domain (66 aa of the N-terminal end; GFP-IP_3K-A-Δact) completely abolished the spinogenic activity of IP_3K-A. Additionally, GFP-IP_3K-A-Δact showed a dominant-negative effect on spine density when compared with the GFP control (Tukey's test, $p < 0.05$) (Fig. 2*D*,*G*), suggesting that the F-actin binding ability of IP_3K-A is essential for spine-forming activity. GFP-IP_3K-A-WT and GFP-IP_3K-A-Δact signals were perfectly merged with F-actin (Fig. 3*A*) and DsRed (supplemental Fig. S8, available at www.jneurosci.org as supplemental material) signals, respectively, indicating that both GFP signals can be used as markers for dendritic protrusion morphology.

Collectively, these data suggest that IP_3K-A is involved in the formation or maintenance of dendritic spines via its ability to interface with the actin cytoskeleton.

IP_3K-A influences actin dynamics

The above results indicated a functional interplay between IP_3K-A and F-actin in the process of dendritic protrusion formation. Indeed, GFP-IP_3K-A colocalizes with postsynaptic F-actin, further suggesting that spine remodeling in neurons by IP_3K-A might be related to actin dynamics (Fig. 3*A*). To examine whether actin reorganization is involved in the IP_3K-A-induced increase in protrusion density, HeLa cells were infected with GFP-IP_3K-A-expressing adenovirus. This heterologous system has two major advantages: (1) F-actin fibers of HeLa cells are clearly resolved, allowing close observation of actin dynamics; and (2) HeLa cells do not express IP_3K-A, eliminating any possible influ-

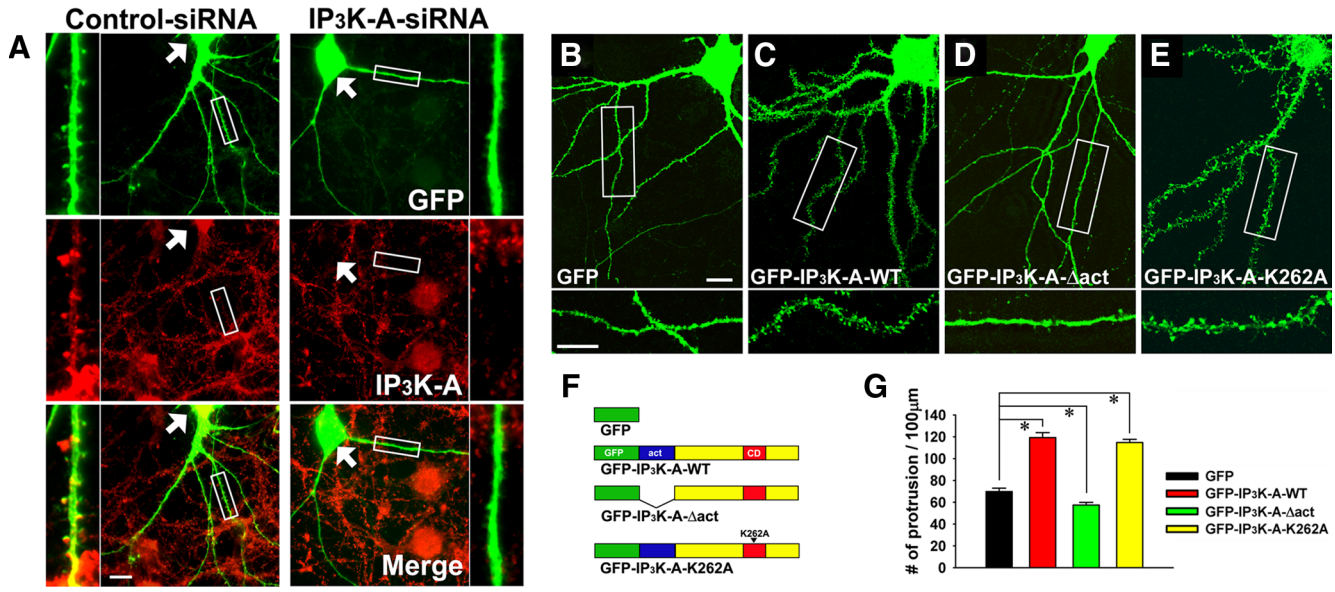

Figure 2. IP_3K-A promotes dendritic spine formation. ***A***, IP_3K-A siRNA transfection (36 h) downregulated the expression of IP_3K-A protein (red signals) and reduced the number of dendritic spines (green signals) of DIV 22 hippocampal neurons. High-magnification views showed that GFP signals of neurons transfected by control siRNA represented normal spine morphology, whereas those of IP_3K-A siRNA-transfected neurons showed a markedly reduced spine density. The arrows indicate the cell bodies of control siRNA- and IP_3K-A siRNA-transfected neurons, showing the absence of IP_3K-A protein in IP_3K-A siRNA-transfected neuron, but not in control siRNA-transfected neuron. Scale bar, 10 μm. ***B–E***, Mature hippocampal neurons (DIV 22) were infected with adenovirus containing GFP or GFP fused to full-length IP_3K-A (GFP-IP_3K-A-WT), or an F-actin-binding domain deletion mutant of IP_3K-A (GFP-IP_3K-A-Δact), or a point mutant form of IP_3K-A (GFP-IP_3K-A-K262A) for 18 h. GFP-IP_3K-A-WT overexpression dramatically increased the density of dendritic protrusions (***C***) compared with control GFP expression (***B***). Overexpressed GFP-IP_3K-A-Δact was diffusely localized in neurons and did not change the morphology of dendritic spines (***D***). Overexpressed GFP-IP_3K-A-K262A, which has no kinase activity, was primarily localized in protrusion heads with a protrusion density similar to that of overexpressed GFP-IP_3K-A-WT (***E***). Scale bar, 10 μm. High-magnification view indicates that overexpressed GFP-IP_3K-A was localized primarily in protrusion heads rather than shafts (***C***). Scale bar, 7 μm. ***F***, The schematic figure indicates the regions of deletion domain or point mutation on IP_3K-A. GFP, Enhanced GFP protein; act, actin-binding domain; CD, catalytic domain; K262A, point mutation at Lys ^{262} to Ala. ***G***, Quantification revealed that the number of dendritic protrusions was significantly increased in neurons with overexpressed GFP-IP_3K-A-WT and GFP-IP_3K-A-K262A, but was decreased by GFP-IP_3K-A-Δact overexpression compared with neurons overexpressing GFP ($F_{(3,201)} = 90.03$; Tukey's test, $^*p < 0.05$). Data are presented as mean ± SEM.

ence of endogenous IP_3K-A. After infection, GFP-IP_3K-A signals completely overlapped with F-actin fiber signals. GFP-IP_3K-A-infected cells also substantially reorganized their F-actin structure, resulting in filopodia-like fiber formation (Fig. 3*B*). The results of these HeLa cell-based assays indicate that a major effect of IP_3K-A is to alter actin dynamics.

IP_3K-A acts as a scaffold for activated Rac1

Because small GTPase proteins are known to be key factors for modulating dendritic spine formation through actin polymerization (Nakayama et al., 2000; Tashiro et al., 2000), we asked whether IP_3K-A interacts with small GTPase proteins. In pull-down assays with rat hippocampal lysate (P2) using GST-IP_3K-A, we found that IP_3K-A interacted with Rac1, but not with RhoA and cdc42 (Fig. 3*C*). Because Rac1 is active when GTP binds to it, but inactive when GDP binds to it (Van Aelst and D'Souza-Schorey, 1997), we asked whether the binding affinity of IP_3K-A for Rac1 is dependent on the activity status of Rac1. To address this issue, GDP- or GTPγs-bound purified Rac1 was used in GST pulldown assays with GST-IP_3K-A. This experiment also allowed us to examine whether IP_3K-A binds directly to Rac1 or not. Interestingly, only GTPγs-bound/activated Rac1 exhibited efficient binding affinity to IP_3K-A (Fig. 3*D*). Furthermore, an immunoprecipitation assay with hippocampal lysate demonstrated that endogenous IP_3K-A was able to bind endogenous Rac1 (Fig. 3*E*). Increased binding between IP_3K-A and Rac1 was observed when GTPγs was added to the lysate, whereas no Rac1 binding was detected in the control group that was precipitated by anti-GST antibody. Interaction between overexpressed IP_3K-A and Rac1 also occurred in a HeLa cell model (supplemental Fig. S3, available at www.jneurosci.org as supplemental material).

Because the catalytic activity of IP_3K-A is not required for efficient spine remodeling, we suspected it may not function as a downstream effector of Rac. Instead, our data indicated that IP_3K-A might serve as a novel scaffold for active Rac1. One hallmark feature of a scaffold is that the binding interaction does not occlude other effectors from binding to Rac1. This predicts that, while bound to IP_3K-A, Rac1 should be able to still bind to downstream effectors such as PAK. To address this question, we examined whether a trimeric complex consisting of IP_3K-A, Rac1, and PAK can exist (Fig. 3*F*). Hippocampal lysates were loaded with either GDP or GTPγs, and the Rac binding domain of PAK (CRIB domain) was used to isolate activated Rac1. As expected, Western blot analysis showed that Rac1 was enriched in GTPγs-treated lysate. Immunoblot analysis of these samples showed IP_3K-A was also coprecipitated by the CRIB pulldown assay, but only in GTPγs-treated lysate that also contained Rac1. These results indicate that complexes containing IP_3K-A and active Rac1 are able to simultaneously bind to Rac effectors such as PAK1.

IP_3K-A regulates dendritic spines through Rac1 activity

The ability of IP_3K-A to scaffold active Rac1 suggests Rac1 may be required for IP_3K-A-induced effects in neurons. Thus, we next examined whether IP_3K-A overexpression effects are dependent on Rac1 activity. When HeLa cells were treated with a Rac1-specific inhibitor [6-*N*-[2-[5-(diethylamino)pentan-2-ylamino]-6-methylpyrimidin-4-yl]-2-methylquinoline-4,6-diamine chlo-

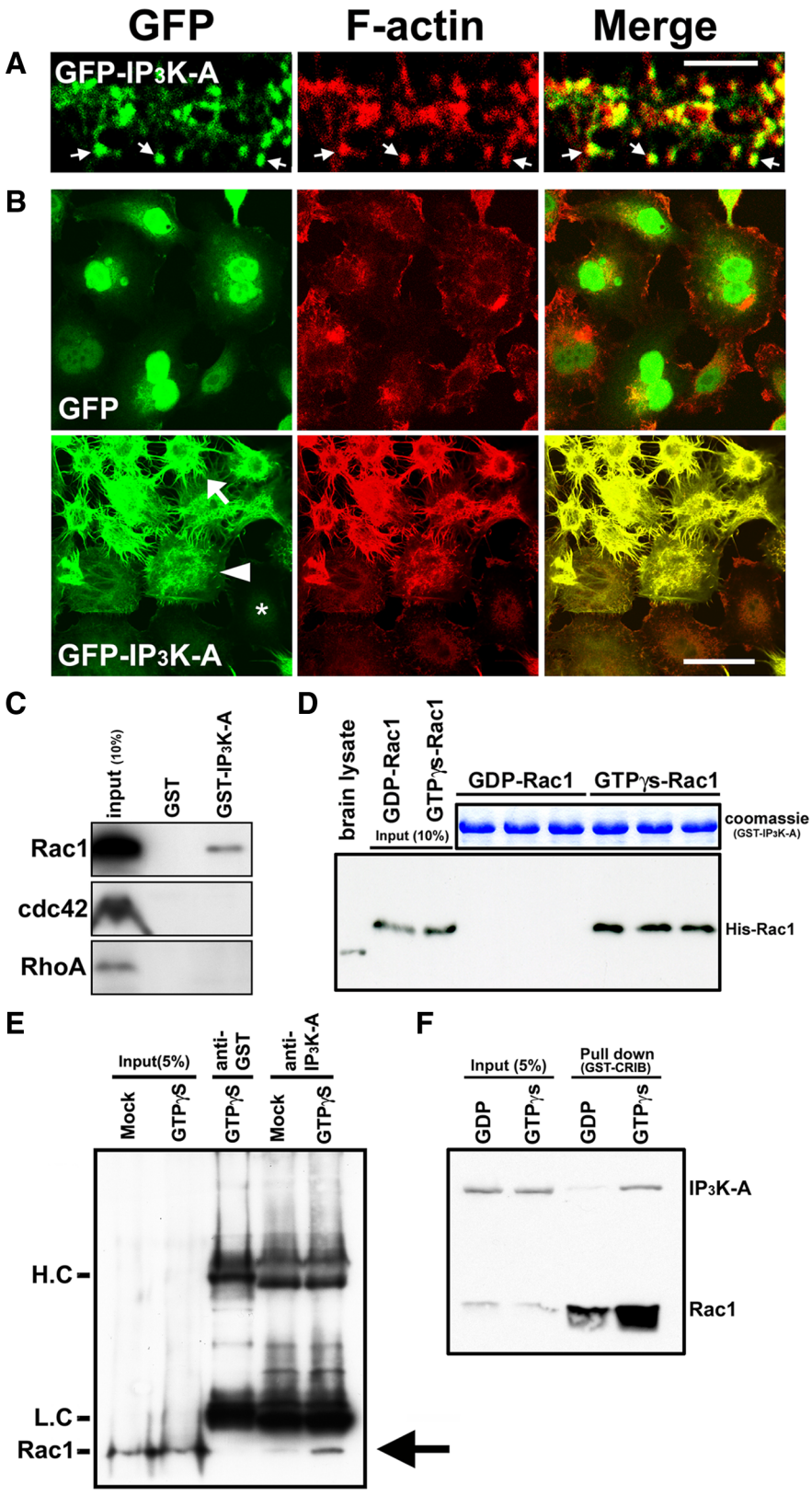

Figure 3. IP_3K-A influences actin dynamics and binds directly to only activated Rac1. ***A***, Overexpressed GFP-IP_3K-A (green) and F-actin (red) signals in neurons merged. The arrows indicate colocalized signals in heads of dendritic protrusions. Scale bar, 5 μm. ***B***, Overexpressed IP_3K-A signals (green) were perfectly merged with F-actin fibers (red) of HeLa cells. GFP-IP_3K-A overexpression increased F-actin fibers, resulting in filopodia-like fiber formation. Note the expression gradient of GFP-IP_3K-A; increased GFP-IP_3K-A expression correlated with increases in filopodial F-actin fibers. Arrow, Strong expression; arrowhead, moderate expression; asterisk, weak expression of GFP-IP_3K-A. Scale bar, 30 μm. ***C***, GST pulldown assay with rat hippocampal P2 fraction by GST-IP_3K-A. IP_3K-A interacted with Rac1, but not with RhoA and cdc42. ***D***, GST pulldown assay with purified His-Rac1 by GST-IP_3K-A. Immunoblotting with anti-Rac1 antibody revealed that IP_3K-A bound to GTPγs-bound purified Rac1 (active Rac1), but did not bind to GDP-bound Rac1 (inactive Rac1). Coomassie staining showed equal loading amounts of GST-IP_3K-A proteins. ***E***, Immunoprecipitation assay with rat hippocampal lysate showed that endogenous IP_3K-A bound to endogenous Rac1. The addition of GTPγs to the lysate increased the amount of precipitated Rac1 compared with non-treated lysate group. Input lanes showed similar loading amounts of lysates. No Rac1 signal was detected in the control group that was precipitated by anti-GST antibody. Similar intensity of heavy and light chain band showed equal loading amounts of IP_3K-A antibody. The arrow indicates Rac1 band. H.C, Heavy chain; L.C, light chain. ***F***, GST-CRIB pulldown assay with GDP- or GTPγs-treated hippocampal lysate. Input lanes showed the equal amount of proteins used in each assays. Pulldown lanes showed that activated Rac1, pulled down with GST-CRIB, was increased by GTPγs treatment. Note that IP_3K-A was co-pulled down with activated Rac1 in GTPγs-treated group.

ride (NSC23766)], filopodia formation induced by GFP-IP_3K-A was blocked, suggesting that Rac1 activity is essential for the effects of IP_3K-A on cellular actin (Fig. 4*A*). To obtain direct evidence of Rac1-mediated IP_3K-A effects on the formation of dendritic protrusions, we treated DIV 22 hippocampal neurons that were infected by GFP-IP_3K-A-expressing adenovirus with NSC23766. After 18 h of treatment, IP_3K-A-induced protrusion formation was partially blocked by the Rac1 inhibitor ($F_{(2,194)} = 65.2$; Scheffé's test, $p < 0.05$) (Fig. 4*B*,*C*). These results indicate that IP_3K-A-induced protrusion formation is dependent on Rac1 activity.

Based on the above results, a question arises as to whether IP_3K-A is involved in regulating the activity status of Rac1 (GDP- or GTP-bound). GST-CRIB pulldown assays using lysates of HeLa cells that had been transfected with GFP-IP_3K-A revealed that overexpressed GFP-IP_3K-A did not affect Rac1 activity, indicating that IP_3K-A is not involved in the exchange of GDP-Rac1 to GTP-Rac1 (supplemental Fig. S4, available at www.jneurosci.org as supplemental material).

LTP induction promotes IP_3K-A/Rac complex formation and synaptic Rac signaling

At the cellular level, LTP induces cytoskeletal remodeling in dendritic spines (Nägerl et al., 2004; Chen et al., 2007). Accordingly, Fukazawa et al. (2003) reported increases in F-actin in the synaptic field by *in vivo* LTP induction. Because we observed enhanced IP_3K-A IR in the synaptic field by LTP induction (Fig. 1), we asked whether Rac activity is enhanced in the synaptic area in which IP_3K-A has accumulated. Because immunostaining for

←

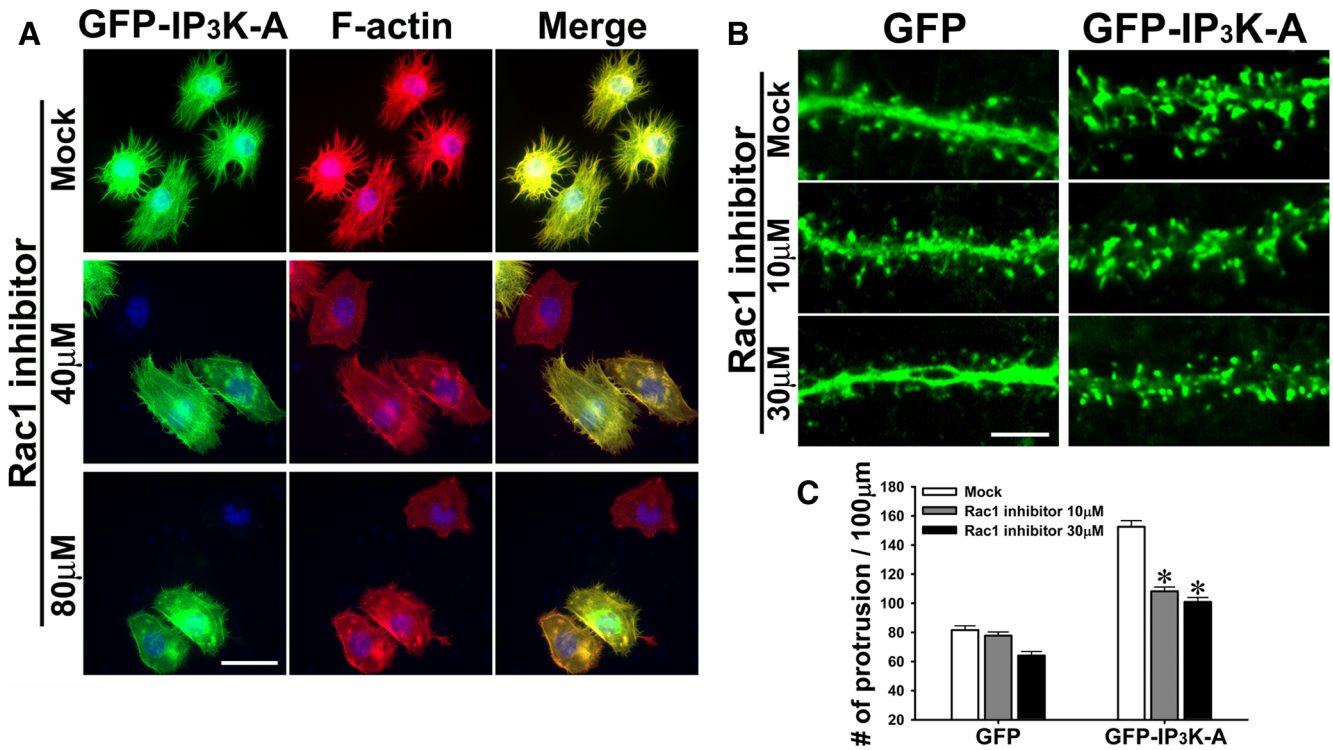

Figure 4. Rac1 activity is essential for IP_3K-A to exert its effects on dendritic spines. ***A***, Rac1-specific inhibitor NSC23766 gradually blocked the IP_3K-A expression-induced formation of filopodia in HeLa cells. After transfection of GFP-IP_3K-A, HeLa cells were incubated for 24 h in medium containing the Rac1 inhibitor. Treatment with 40 μM NSC23766 mostly inhibited, and 80 μM treatment completely inhibited, the filopodia formation effect of IP_3K-A. Scale bar, 30 μm. ***B***, Treatment with NSC23766 (10 or 30 μM) mostly prevented IP_3K-A overexpression from inducing formation of protrusions in DIV 22 hippocampal neurons. Scale bar, 7 μm. ***C***, Quantification revealed that the increased dendritic protrusion number induced by IP_3K-A overexpression was significantly inhibited by NSC23766 treatment. ($F_{(2,194)} = 65.2$; Scheffé's test, $^*p < 0.05$). Data are presented as mean ± SEM.

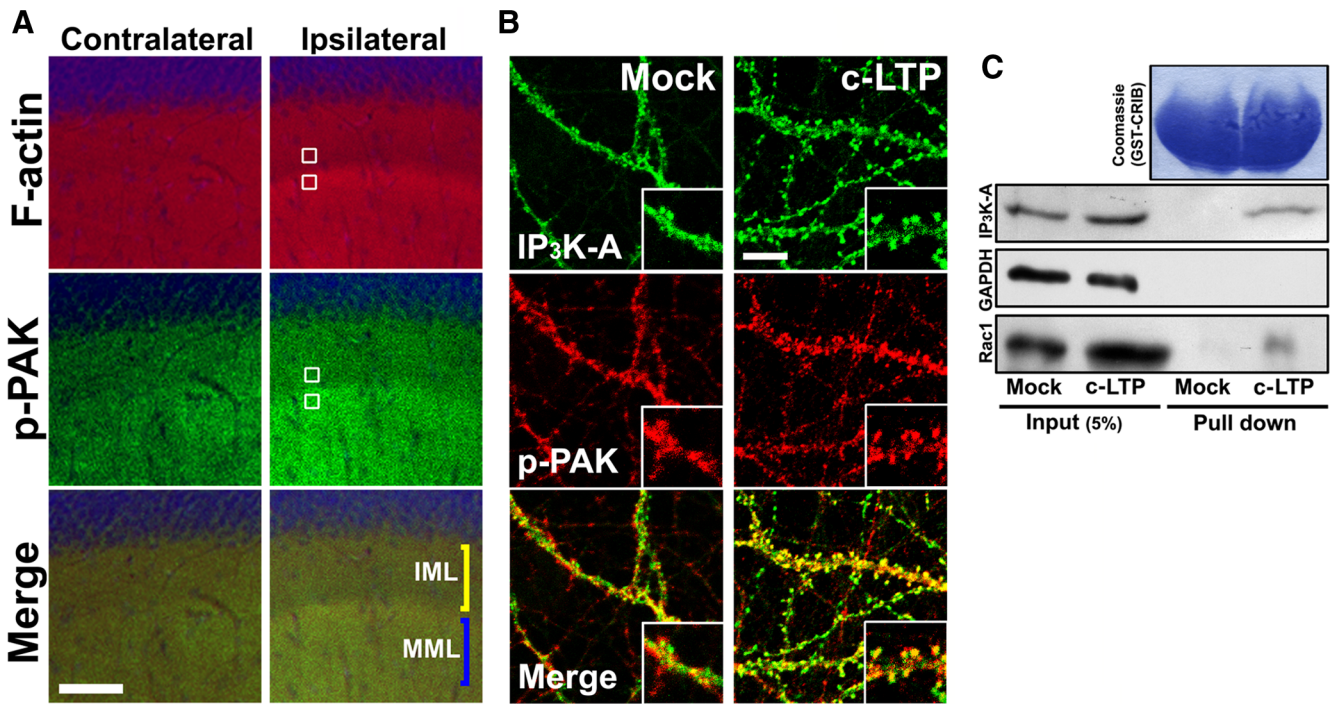

Figure 5. LTP induction activates Rac1 downstream events in dendritic spines. ***A***, Distribution of p-PAK in DG after *in vivo* LTP induction. One hour after last tetanus, p-PAK as well as F-actin had accumulated in spine-rich field of DG (MML) only in the LTP-induced side. The white squares indicate the measure points for immunoreactivity. Scale bar, 100 μm. ***B***, Representative images showing c-LTP-induced targeting of IP_3K-A along with p-PAK into dendritic spines. High-magnification views showed colocalization of p-PAK with IP_3K-A. Scale bar, 10 μm. ***C***, GST-CRIB pulldown assay with c-LTP-induced P2 fraction of neurons. Input lanes showed that total Rac1 as well as IP_3K-A in synaptosome seemed to be slightly increased in LTP-induced neurons, but levels of the control protein GAPDH did not seem to be different between the two groups. Pulldown lanes showed that activated Rac1 (GTP-Rac1), which was pulled down with GST-CRIB, was increased in LTP-induced neurons compared with that in the nontreated control group. IP_3K-A was pulled down with activated Rac1. Coomassie staining showed equal loading amounts of GST-CRIB proteins.

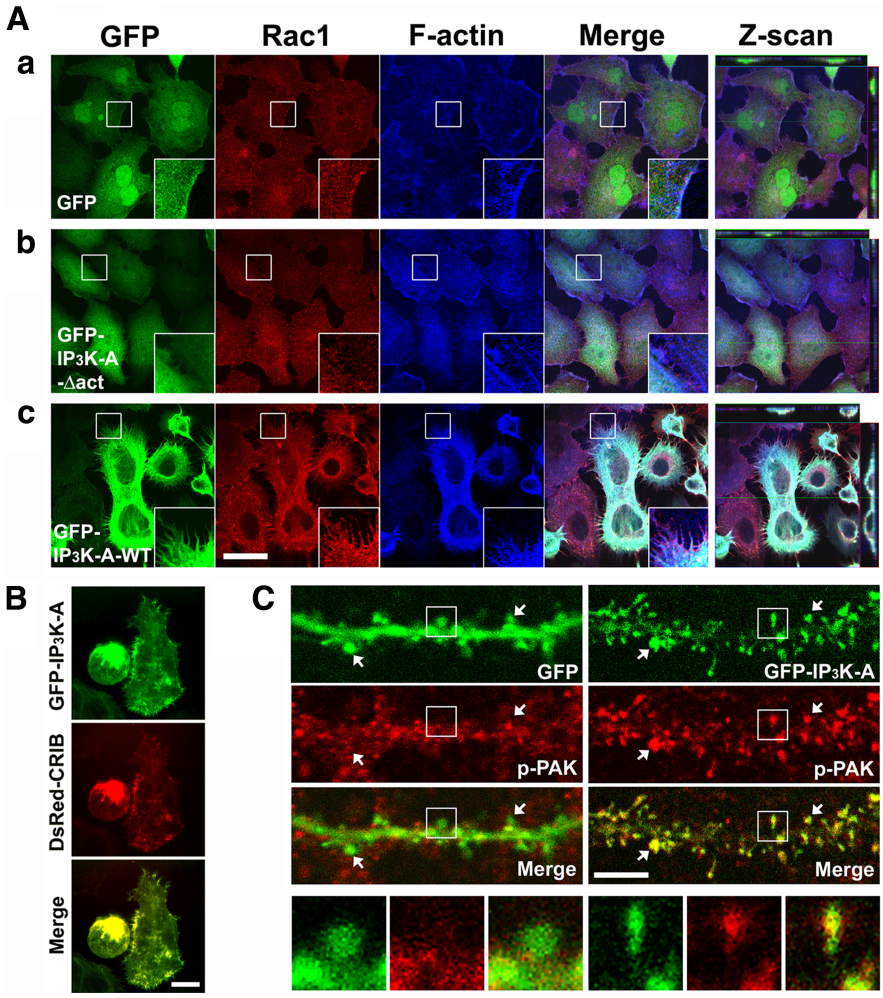

Figure 6. IP_3K-A recruits activated Rac1 onto F-actin fibers. ***Aa***, When HeLa cells were infected by GFP-containing adenoviruses, Rac1 signals were evenly distributed in cells. ***Ab***, Similar to GFP-infected cells, when infected by GFP-IP_3K-A-Δact-containing adenoviruses, Rac1 signals rarely merged with F-actin signals. ***Ac***, When infected by GFP-IP_3K-A-WT, a large part of the Rac1 signal merged with the F-actin fiber signal. *Z*-scan image showed colocalization among Rac1, F-actin, and GFP-IP_3K-A-WT. Scale bar, 30 μm. ***B***, DsRed-CRIB, an activated Rac1-binding domain from PAK1, was colocalized with GFP-IP_3K-A-WT in HeLa cells. Scale bar, 10 μm. ***C***, The majority of p-PAK IRs was accumulated in heads of dendritic protrusions together with overexpressed full-length GFP-IP_3K-A (right panels) compared with GFP-vector-expressing neuron (left panels). The arrows indicate heads of dendritic protrusions. Scale bar, 10 μm.

activated Rac is not currently available, we instead tracked the phosphorylated PAK (p-PAK), a product of activated Rac. As was observed for IP_3K-A (Fig. 1*A*), p-PAK and F-actin were observed to be more accumulated in the synaptic field of the LTP-induced hemisphere than in the contralateral side (Fig. 5*A*) (F-actin: $t = 8.95$, $df = 6$, $p < 0.0001$; p-PAK: $t = 7.05$, $df = 6$, $p < 0.0001$). In fact, total PAK1 was also accumulated in the synaptic field by LTP induction (supplemental Fig. S5, available at www.jneurosci.org as supplemental material), suggesting that this Rac signaling pathway may be augmented. Furthermore, GST-CRIB pulldown assays with the synaptosomal (P2) fraction from c-LTP-induced hippocampal neurons demonstrated that the activated Rac1 pulled down with GST-CRIB was increased in c-LTP-induced neurons compared with that in the nontreated control group. Importantly, IP_3K-A was pulled down together with activated Rac1, showing this signaling complex is organized downstream of synaptic activity (Fig. 5*C*). Immunocytochemical assay also showed that p-PAK IR overlapped with spine-targeted IP_3K-A IR (Fig. 5*B*). Densitometry analysis revealed that more p-PAK IRs were accumulated in dendritic spines by c-LTP induction ($t = 4.03$; $df = 24$; $p < 0.0001$), corresponding to the report of Chen et al. (2007) describing the p-PAK accumulation in the CA1 dendritic spines by LTP induction using rat brain slices. Because isolated dentate granule neurons cannot be cultured, we examined the localization of IP_3K-A in CA neurons as the best available proxy. These results likely hold true in both neuronal types since IP_3K-A is expressed equally in the CA1 and DG. Together, these results suggest IP_3K-A acts as an activity-dependent scaffold for activated Rac in dendritic spines, at which Rac downstream events are stimulated on neural activation.

IP_3K-A recruits activated Rac onto F-actin fibers

Based on the above observations, we hypothesized that IP_3K-A recruits activated Rac1 onto the F-actin in the dendrites and spines after neuronal activation. To test this hypothesis, first we infected HeLa cells with adenoviruses containing full-length IP_3K-A (GFP-IP_3K-A-WT) or GFP-IP_3K-A-Δact or GFP vector, then examined the localization of Rac1. Under normal conditions (GFP vector expression), Rac1 IR was diffusely localized in the cytoplasm and was not associated with F-actin (Fig. 6*Aa*). However, after GFP-IP_3K-A-WT overexpression, a majority of Rac1-IR and GFP-IP_3K-A-WT signals were colocalized with augmented F-actin fibers (Fig. 6*Ac*), whereas Rac1 IR was diffusely localized in cytoplasm when GFP-IP_3K-A-Δact was overexpressed (Fig. 6*Ab*). *z*-axis image analysis indicated the colocalization of the three signals (F-actin, Rac1, and IP_3K-A-WT) in IP_3K-A-WT overexpressed cells. Because both GFP-IP_3K-A-WT and GFP-IP_3K-A-Δact can bind to Rac1 (supplemental Fig. S6, available at www.jneurosci.org as supplemental material), this difference is not attributable to differential binding ability. Thus, we reasoned that F-actin binding ability of IP_3K-A is required for the targeting of Rac1 onto the actin cytoskeleton. Moreover, cotransfection of GFP-IP_3K-A and DsRed-CRIB into HeLa cells revealed that IP_3K-A indeed recruits activated Rac onto the actin fibers (Fig. 6*B*). Furthermore, p-PAK IRs were dramatically merged with overexpressed GFP-IP_3K-A signals, which are localized on the F-actin in the head of dendritic protrusions (Figs. 3*A*, 6C), suggesting that IP_3K-A-dependent targeting of activated Rac onto F-actin cytoskeleton also occurs in neurons.

In vivo impairment of activity-dependent accumulation of PAK1/F-actin and synaptic plasticity in IP_3K-A knock-out mice

The combined results so far indicate a model whereby IP_3K-A plays an important role in synaptic targeting of active Rac. Our *in vitro* data predict that, in the absence of IP_3K-A, there may be alterations to the developmental course leading to synapse for-

mation. Golgi staining followed by camera lucida analyses with young KO mice (4 weeks of age) revealed a significantly decreased density of dendritic spines in DG neurons ($F_{(3,14)} = 125.2$; Scheffé's test, $p < 0.05$). However, the spine density recovered to the WT value in 8-week-old KO mice (supplemental Fig. S7, available at www.jneurosci.org as supplemental material). These observations suggest a retardation of the spine development in KO mice, which is rescued by an unknown compensatory mechanism at later time points. Nonetheless, these data are in agreement with our *in vitro* data implicating IP_3K-A function during active spinogenesis.

Our model also predicts that, in the absence of IP_3K-A, synaptic activation of Rac-dependent pathways and actin remodeling may be blunted. To test this, we examined whether adult IP_3K-A KO mice have defects in neural activation-induced accumulation of F-actin and PAK1 in the synaptic area of DG. After tetanic stimulation in the perforant path of 3-month-old mice, we observed less PAK1 and F-actin in the middle molecular layer (MML) and outer molecular layer (OML) of the DG in KO mice when compared with littermate controls ($t = 43.81$, df = 4, $p < 0.0001$ for PAK1; $t = 8.50$, df = 4, $p < 0.001$ for F-actin) (Fig. 7*A*,*B*), suggesting that IP_3K-A plays an essential role in activated Rac targeting as well as in activity-dependent actin dynamics in DG neurons *in vivo*.

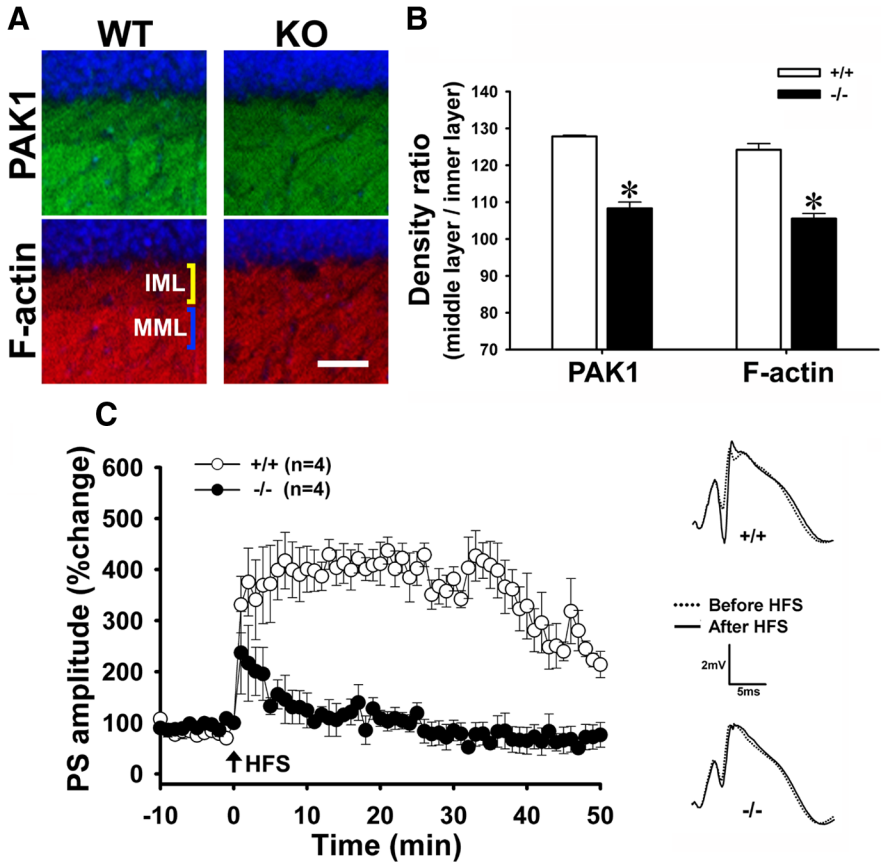

Figure 7. IP_3K-A knock-out mice show defects in LTP and actin dynamics in dentate gyrus. ***A***, Less PAK1 and F-actin was observed in the MML and OML of the DG in KO mice compared with WT mice. ***B***, Densitometry analyses revealed the defect of KO mice in PAK1 and F-actin accumulation in the synaptic field of DG (MML) by neural activation (PAK1: $t = 43.81$, df = 4, $^*p < 0.0001$; F-actin: $t = 8.50$, df = 4, $^*p < 0.001$). Data are presented as mean ± SEM. ***C***, *In vivo* LTP experiments of DG-perforant path showed that LTP of the population spike was disrupted in KO mice when compared with WT littermate mice (363.4 ± 8.6% for WT; 102.6 ± 5.9% for KO; paired *t* test; $t = 29.5$, df = 49, $p < 0.0001$). Data are mean ± SEM population spikes. Slopes are expressed as a percentage of the baseline recordings made 10 min before HFS. The right panel shows representative waveforms of both genotypes.

To elucidate the physiological significance of IP_3K-A in adult brains, we next investigated the synaptic plasticity in IP_3K-A KO mice. Previously, Jun et al. (1998) reported that the hippocampal slices of IP_3K-A KO mice showed enhanced LTP in CA1 region. Additionally, there was a slight, but distinct disruption of DG LTP in KO mice during first 30 min even though the magnitude of potentiation was <0.15 mV induced by 100 Hz stimulations. To examine plasticity in the DG in a more physiologic context, we used an *in vivo* LTP induction and measurement method. For this, we induced LTP in the anesthetized mice (10 weeks of age) using stereotactically placed probes. LTP was induced by high-frequency stimulation (HFS) in perforant path–DG synapses. Notably, IP_3K-A KO mice exhibited disrupted LTP compared with WT littermate mice. The magnitude of potentiation after HFS was enhanced 363.4 ± 8.6% or 102.6 ± 5.9% over the initial baseline average in the WT or KO mice, respectively (Fig. 7*C*). The difference of the enhancement between the two genotypes was statistically significant (paired *t* test; $t = 29.5$, df = 49, $p < 0.0001$). Although KO mice also showed inductions of population spikes by HFS (72% of WT mice), the induced potentiations were not maintained over 20 min, suggesting the possibility that rapid remodeling of actin by IP_3K-A is important to the maintenance of synaptic plasticity *in vivo*. A previous report showed that there was no difference in paired-pulse facilitation in perforant path between WT and KO (Jun et al., 1998). Basically, in addition, IP_3K-A does not express in axon including presynapse (data not shown), suggesting that IP_3K-A may not be essential for axonal input.

IP_3K-A knock-out mice show defects in memory performances

Previously, it was reported that there was no significant difference in escape latency between IP_3K-A KO and WT mice in the Morris water maze test (Jun et al., 1998); we also confirmed this result (data not shown). However, we observed that IP_3K-A KO mice have augmented fear levels compared with WT mice (unpublished observations). Because Morris water maze may evoke fear-related responses, a high level of fear in KO mice should enhance the driving force to search for the hidden platform, complicating the interpretation of these results. Thus, we tested the capability for memory formation in IP_3K-A KO mice using alternative hippocampal-dependent memory tasks that are less influenced by fear motivations. We first performed an object recognition test. In this test, mice are instinctively interested in a novel object rather than a familiar one. If a mouse remembers the object that has been explored before, it will normally prefer to explore and contact a new object more frequently. As expected, WT mice recognized and spent more time exploring the new object in a 24 h choice test. In contrast, IP_3K-A KO mice did not recognize

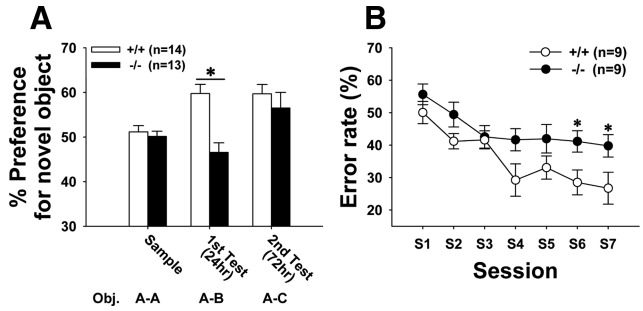

Figure 8. IP_3K-A knock-out mice show defects in synaptic plasticity and memory performances. ***A***, IP_3K-A KO mice showed defects in novel object recognition. One day after a sample trial of an object recognition test, WT mice spent more time exploring a novel object (object B); however, exploration of a novel object by KO mice remained at the chance level (Scheffé's test, $*p < 0.05$). At a second choice test (exposure three times to object A), KO mice spent substantially more time on the new object C. Obj, Object. Data are presented as mean ± SEM. ***B***, IP_3K-A KO mice showed defects in spatial learning tasks. The error rates of KO mice at session 6 and 7 of the radial arm maze test were significantly higher than those of WT mice ($*p < 0.05$). Data are presented as mean ± SEM.

the novel object and spent similar amounts of time exploring each object (Scheffé's test, $p < 0.05$) (Fig. 8*A*) (for additional statistical analysis, see supplemental material, available at www.jneurosci.org as supplemental material). Thus, KO mice have a reduced ability to process novel object recognition memory. A 72 h choice was subsequently performed, using the familiar versus yet another novel object. In this trial, in which both genotypes have been exposed to the familiar object on three occasions, both WT and KO mice recognized the novel object. These data indicate that, with an additional trial, the IP_3K-A KO mice can distinguish the familiar versus novel object and confirm that these mice retain novelty-seeking behavior. Importantly, neophobic responses to the objects did not confound the behavior in either cohort, as the total number of touches on objects was not different between either genotype (data not shown).

Memory deficits were also noted in an independent assay to evaluate spatial memory using the radial arm maze test. In this task, mice were required to remember previously visited maze arms extending from a central starting platform to get rewards. Spatial memory errors were measured as the number of visits to the same arm more than once, in which the reward had already been obtained. Interestingly, both WT and KO mice improved their error rate in the first three trials. After this point, WT mice continued to improve, whereas KO mice did not. Statistical analyses with ANOVA (repeated measures) followed by Bonfferoni's correction revealed that the KO mice were impaired in spatial memory on sessions 6 and 7 ($p < 0.05$) (Fig. 8*B*) (for additional statistical analysis, see supplemental material, available at www.jneurosci.org as supplemental material). These results suggest that the spatial memory of IP_3K-A KO mice was also impaired in this test.

Discussion

In the present study, we identified a novel function of IP_3K-A that regulates activity-dependent remodeling of dendritic spine actin by scaffolding active Rac. We found that IP_3K-A is translocated to dendritic spines by neural activation, in which it recruits and anchors activated Rac to the actin cytoskeleton. Our *in vivo* and *in vitro* data may provide new insights into the site-specific and time-dependent signaling mechanisms of synaptic plasticity, which appears to be important for the processes of memory formation.

The plasticity-dependent localization of IP_3K-A in dendritic spines

We demonstrated here the targeting of IP_3K-A in dendritic spines follows LTP induction. Previously, it was reported that treatment of cultured neurons with glutamate or NMDA diminishes IP_3K-A levels in dendritic spine heads (Schell and Irvine, 2006). In agreement with this, we also observe a similar loss of IP_3K-A from spine heads after 100 μM glutamate treatment; yet with this treatment, the spines eventually collapsed (data not shown). Accumulating evidence suggests that direct treatment of brain slices with NMDA produces long-term depression-like phenomena (Lee et al., 1998), which promote the shrinkage of spines (Zhou et al., 2004). Furthermore, we also previously showed that aberrant neuronal activations by chemical reagents (kainic acid) or electric stimulation (electroconvulsive shock) reduce the expression of IP_3K-A (Kim et al., 1994; Sun et al., 2006). Because these conditions reduce synaptic efficacy and induce amnesia (Squire and Spanis, 1984; Holmes, 1991), these results collectively suggested that the expression and localization of IP_3K-A might be dynamically regulated by neuronal plasticity. Our current study evaluated the dynamics of IP_3K-A localization after LTP induction. After *in vivo* and *in vitro* c-LTP induction, IP_3K-A dramatically accumulated in the synaptic area, demonstrating that the localization of IP_3K-A is regulated by neuronal activity. Therefore, the localization of IP_3K-A in the dendrites appears to be intimately paired with mechanisms of synaptic plasticity *in vivo*.

IP_3K-A-induced remodeling of dendritic spines uses a novel kinase-independent mechanism

Overexpression of IP_3K-A in neurons markedly increased the number of dendritic protrusions, whereas knockdown of IP_3K-A expression reduced the number of these protrusions. Together, these results suggest that IP_3K-A can modulate structural reorganization of dendritic spines. Until now, the only known role of IP_3K-A was its kinase activity, which phosphorylates IP_3 to IP_4 (Irvine et al., 1986). IP_4 is known to regulate calcium influx from the endoplasmic reticulum in combination with IP_3 (Hermosura et al., 2000). Because intraspine calcium is essential for the control of actin dynamics and spine morphology (Oertner and Matus, 2005), it was natural to assume that the mechanism of IP_3K-A to modify actin dynamics is related to its catalytic activity. Surprisingly, the present results exclude this idea. Overexpression of IP_3K-A-K262A, a point mutant lacking catalytic activity, recapitulated the spine-forming effect of normal IP_3K-A, suggesting that the catalytic activity of IP_3K-A is not essential for spine formation. In line with our result, cytoskeletal reorganization induced by IP_3K-A overexpression was observed in H1299 cells, independent of its catalytic activity (Windhorst et al., 2008). Furthermore, Jun et al. (1998) reported that the responses of intracellular calcium levels to glutamate treatment in the neurons of IP_3K-A KO mice were similar to those of neurons in WT mice, adding to the likelihood that the kinase activity of IP_3K-A is not relevant to its function in spines.

Although IP_3K-A lacking catalytic activity could still induce spine formation, deletion of the actin-binding domain of IP_3K-A completely eliminated this effect, indicating that the spine-forming activity of IP_3K-A is related to its ability to interact with F-actin. Because IP_3K-A was found to be a direct binding partner of the active form of Rac1, and inhibition of Rac1 partially blocked the spine-forming activity of IP_3K-A, we hypothesized that IP_3K-A may play an anchoring role between activated Rac and actin cytoskeleton in dendritic spines.

Rac signaling remodels F-actin structures, producing a specific morphology in many types of cells, including neurons (Hering and Sheng, 2001; Etienne-Manneville and Hall, 2002). Constitutively active Rac disrupts normal spine morphology of neurons, causing a net increase of dendritic protrusions. Conversely, dominant-negative Rac causes a progressive reduction of the number of spines (Nakayama et al., 2000; Tashiro et al., 2000), indicating that Rac activity is important for the maintenance of spine density. The regulation of Rac activity status (GTP–GDP exchange) by GEFs and GAPs (GTPase-activating proteins) is crucial for activity-dependent synaptic remodeling (Van Aelst and D'Souza-Schorey, 1997). For instance, Rac-GEFs βPIX, Tiam1, and kalirin-7 are localized within the spine head, and their activity is regulated by synaptic activity (Penzes et al., 2001; Tolias et al., 2005; Saneyoshi et al., 2008). In addition to Rac activation, the anchoring and targeting of activated Rac to "hot spots" of actin remodeling may be required to promote actin dynamics-mediated spine formation. Additionally, if the positioning of activated Rac is restricted to preexisting spines, it would be difficult to explain the phenomena of the formation of new spines from the dendritic shaft by the Rac pathway. We propose in this study that IP_3K-A recruits activated Rac to F-actin-rich domains in which Rac signaling is required for mechanisms of synaptic plasticity. This is supported by our findings that, after LTP induction, p-PAK accumulated with an IP_3K-A/F-actin complex in the synaptic area in adult rat DG. Importantly, IP_3K-A KO mice showed a clear reduction of PAK1 and F-actin accumulation in the synaptic field. These data highlight the possibility that IP_3K-A plays an essential scaffolding role in support of Rac signaling events by localizing activated Rac within the actin-rich spines of neurons.

Impairment of synaptic plasticity and memory formation in IP_3K-A knock-out mice

Consistent with the reduced PAK1 and F-actin accumulations, we observed in IP_3K-A KO mice, *in vivo* LTP was also greatly impaired, suggesting that the IP_3K-A/Rac/F-actin complex we identified is essential for synaptic plasticity *in vivo*.

These defects were also manifested by behavioral impairments in the IP_3K-A KO mice. Object recognition and radial arm maze tests consistently demonstrated the impairment of hippocampal-dependent memory formation in IP_3K-A KO mice. Recognition memory is associated with the function of the hippocampal formation regions in humans, monkeys, and rodents (Myhrer, 1988; Reed and Squire, 1997; Zola et al., 2000). For example, rats seem to be unable to recognize novelty when hippocampal perforant path projection is disrupted (Myhrer, 1988). In present study, IP_3K-A KO mice showed a deficit in remembering the object seen the day before the testing, indicating reduced ability of recognition memory of KO mice.

We also used the radial arm maze test, in which the ability to master the task being tested is also dependent on the hippocampal formation, including the DG (McNaughton et al., 1989). Although the radial arm maze test can evaluate the capacity of spatial working memory, this task also requires reference memory (Satoh et al., 2007). Interestingly, IP_3K-A KO mice showed no difference in radial arm maze test error rate compared with WT animals in the first three sessions, suggesting that there was no specific working memory deficit during that early period. Yet, whereas WT mice continued to improve their error rate after session 3, KO mice did not. Therefore, it is possible that the spatial memory deficit of KO mice in late phases may be caused by the retardation of working memory improvement, or by differences in reference memory. In either scenario, our analysis using both the novel object recognition and radial arm tests are consistent with deficits in learning and memory as a consequence of the loss of IP_3K-A-dependent pathways.

In summary, we define a previously unknown mechanism to scaffold active Rac to spines in response to plasticity-inducing stimuli. Our data indicate that this mechanism is essential for *in vivo* Rac signaling pathways, synaptic plasticity, and aspects of hippocampal-dependent learning and memory.

References

Bliss TV, Collingridge GL, Morris RG (2003) Introduction. Long-term potentiation and structure of the issue. Philos Trans R Soc Lond B Biol Sci 358:607–611.

Bonhoeffer T, Yuste R (2002) Spine motility. Phenomenology, mechanisms, and function. Neuron 35:1019–1027.

Chen LY, Rex CS, Casale MS, Gall CM, Lynch G (2007) Changes in synaptic morphology accompany actin signaling during LTP. J Neurosci 27:5363–5372.

Choi KY, Kim HK, Lee SY, Moon KH, Sim SS, Kim JW, Chung HK, Rhee SG (1990) Molecular cloning and expression of a complementary DNA for inositol 1,4,5-trisphosphate 3-kinase. Science 248:64–66.

Dailey ME, Smith SJ (1996) The dynamics of dendritic structure in developing hippocampal slices. J Neurosci 16:2983–2994.

Engert F, Bonhoeffer T (1999) Dendritic spine changes associated with hippocampal long-term synaptic plasticity. Nature 399:66–70.

Etienne-Manneville S, Hall A (2002) Rho GTPases in cell biology. Nature 420:629–635.

Fukazawa Y, Saitoh Y, Ozawa F, Ohta Y, Mizuno K, Inokuchi K (2003) Hippocampal LTP is accompanied by enhanced F-actin content within the dendritic spine that is essential for late LTP maintenance in vivo. Neuron 38:447–460.

Hering H, Sheng M (2001) Dendritic spines: structure, dynamics and regulation. Nat Rev Neurosci 2:880–888.

Hermosura MC, Takeuchi H, Fleig A, Riley AM, Potter BV, Hirata M, Penner R (2000) InsP4 facilitates store-operated calcium influx by inhibition of InsP3 5-phosphatase. Nature 408:735–740.

Holmes GL (1991) The long-term effects of seizures on the developing brain: clinical and laboratory issues. Brain Dev 13:393–409.

Irvine RF, Letcher AJ, Heslop JP, Berridge MJ (1986) The inositol tris/tetrakisphosphate pathway—demonstration of Ins(1,4,5)P3 3-kinase activity in animal tissues. Nature 320:631–634.

Jun K, Choi G, Yang SG, Choi KY, Kim H, Chan GC, Storm DR, Albert C, Mayr GW, Lee CJ, Shin HS (1998) Enhanced hippocampal CA1 LTP but normal spatial learning in inositol 1,4,5-trisphosphate 3-kinase(A)-deficient mice. Learn Mem 5:317–330.

Kennedy MB, Beale HC, Carlisle HJ, Washburn LR (2005) Integration of biochemical signalling in spines. Nat Rev Neurosci 6:423–434.

Kim H, Ko JP, Kang UG, Park JB, Kim HL, Lee YH, Kim YS (1994) Electroconvulsive shock reduces inositol 1,4,5-trisphosphate 3-kinase mRNA expression in rat dentate gyrus. J Neurochem 63:1991–1994.

Kim HT, Kim IH, Lee KJ, Lee JR, Park SK, Chun YH, Kim H, Rhyu IJ (2002) Specific plasticity of parallel fiber/Purkinje cell spine synapses by motor skill learning. Neuroreport 13:1607–1610.

Kim IH, Park SK, Sun W, Kang Y, Kim HT, Kim H (2004) Spatial learning enhances the expression of inositol 1,4,5-trisphosphate 3-kinase A in the hippocampal formation of rat. Brain Res Mol Brain Res 124:12–19.

Lee HK, Kameyama K, Huganir RL, Bear MF (1998) NMDA induces long-term synaptic depression and dephosphorylation of the GluR1 subunit of AMPA receptors in hippocampus. Neuron 21:1151–1162.

Leuner B, Falduto J, Shors TJ (2003) Associative memory formation increases the observation of dendritic spines in the hippocampus. J Neurosci 23:659–665.

Lin B, Kramár EA, Bi X, Brucher FA, Gall CM, Lynch G (2005) Theta stimulation polymerizes actin in dendritic spines of hippocampus. J Neurosci 25:2062–2069.

Luo L (2002) Actin cytoskeleton regulation in neuronal morphogenesis and structural plasticity. Annu Rev Cell Dev Biol 18:601–635.

Mailleux P, Takazawa K, Erneux C, Vanderhaeghen JJ (1991) Inositol 1,4,5-trisphosphate 3-kinase mRNA: high levels in the rat hippocampal CA1

pyramidal and dentate gyrus granule cells and in cerebellar Purkinje cells. J Neurochem 56:345–347.
Maletic-Savatic M, Malinow R, Svoboda K (1999) Rapid dendritic morphogenesis in CA1 hippocampal dendrites induced by synaptic activity. Science 283:1923–1927.
Matus A, Ackermann M, Pehling G, Byers HR, Fujiwara K (1982) High actin concentrations in brain dendritic spines and postsynaptic densities. Proc Natl Acad Sci U S A 79:7590–7594.
McNaughton BL, Barnes CA, Meltzer J, Sutherland RJ (1989) Hippocampal granule cells are necessary for normal spatial learning but not for spatially-selective pyramidal cell discharge. Exp Brain Res 76:485–496.
Myhrer T (1988) Exploratory behavior and reaction to novelty in rats with hippocampal perforant path systems disrupted. Behav Neurosci 102: 356–362.
Nägerl UV, Eberhorn N, Cambridge SB, Bonhoeffer T (2004) Bidirectional activity-dependent morphological plasticity in hippocampal neurons. Neuron 44:759–767.
Nakayama AY, Harms MB, Luo L (2000) Small GTPases Rac and Rho in the maintenance of dendritic spines and branches in hippocampal pyramidal neurons. J Neurosci 20:5329–5338.
Oertner TG, Matus A (2005) Calcium regulation of actin dynamics in dendritic spines. Cell Calcium 37:477–482.
Penzes P, Johnson RC, Sattler R, Zhang X, Huganir RL, Kambampati V, Mains RE, Eipper BA (2001) The neuronal Rho-GEF Kalirin-7 interacts with PDZ domain-containing proteins and regulates dendritic morphogenesis. Neuron 29:229–242.
Penzes P, Beeser A, Chernoff J, Schiller MR, Eipper BA, Mains RE, Huganir RL (2003) Rapid induction of dendritic spine morphogenesis by trans-synaptic ephrinB-EphB receptor activation of the Rho-GEF kalirin. Neuron 37:263–274.
Purpura DP (1974) Dendritic spine "dysgenesis" and mental retardation. Science 186:1126–1128.
Reed JM, Squire LR (1997) Impaired recognition memory in patients with lesions limited to the hippocampal formation. Behav Neurosci 111: 667–675.
Saneyoshi T, Wayman G, Fortin D, Davare M, Hoshi N, Nozaki N, Natsume T, Soderling TR (2008) Activity-dependent synaptogenesis: regulation by a CaM-kinase kinase/CaM-kinase I/betaPIX signaling complex. Neuron 57:94–107.
Satoh Y, Endo S, Ikeda T, Yamada K, Ito M, Kuroki M, Hiramoto T, Imamura O, Kobayashi Y, Watanabe Y, Itohara S, Takishima K (2007) Extracellular signal-regulated kinase 2 (ERK2) knockdown mice show deficits in long-term memory; ERK2 has a specific function in learning and memory. J Neurosci 27:10765–10776.
Schell MJ, Irvine RF (2006) Calcium-triggered exit of F-actin and IP(3) 3-kinase A from dendritic spines is rapid and reversible. Eur J Neurosci 24:2491–2503.
Schell MJ, Erneux C, Irvine RF (2001) Inositol 1,4,5-trisphosphate 3-kinase A associates with F-actin and dendritic spines via its N terminus. J Biol Chem 276:37537–37546.
Segal M (2005) Dendritic spines and long-term plasticity. Nat Rev Neurosci 6:277–284.
Squire LR, Spanis CW (1984) Long gradient of retrograde amnesia in mice: continuity with the findings in humans. Behav Neurosci 98:345–348.
Star EN, Kwiatkowski DJ, Murthy VN (2002) Rapid turnover of actin in dendritic spines and its regulation by activity. Nat Neurosci 5:239–246.
Sun W, Kang Y, Kim IH, Kim EH, Rhyu IJ, Kim HJ, Kim H (2006) Inhibition of rat brain inositol 1,4,5-trisphosphate 3-kinase A expression by kainic acid. Neurosci Lett 392:181–186.
Tashiro A, Minden A, Yuste R (2000) Regulation of dendritic spine morphology by the rho family of small GTPases: antagonistic roles of Rac and Rho. Cereb Cortex 10:927–938.
Togashi S, Takazawa K, Endo T, Erneux C, Onaya T (1997) Structural identification of the myo-inositol 1,4,5-trisphosphate-binding domain in rat brain inositol 1,4,5-trisphosphate 3-kinase. Biochem J 326:221–225.
Tolias KF, Bikoff JB, Burette A, Paradis S, Harrar D, Tavazoie S, Weinberg RJ, Greenberg ME (2005) The Rac1-GEF Tiam1 couples the NMDA receptor to the activity-dependent development of dendritic arbors and spines. Neuron 45:525–538.
Van Aelst L, D'Souza-Schorey C (1997) Rho GTPases and signaling networks. Genes Dev 11:2295–2322.
Windhorst S, Blechner C, Lin HY, Elling C, Nalaskowski M, Kirchberger T, Guse AH, Mayr GW (2008) Ins(1,4,5)P3 3-kinase-A overexpression induces cytoskeletal reorganization via a kinase-independent mechanism. Biochem J 414:407–417.
Xie Z, Huganir RL, Penzes P (2005) Activity-dependent dendritic spine structural plasticity is regulated by small GTPase Rap1 and its target AF-6. Neuron 48:605–618.
Yuste R, Bonhoeffer T (2001) Morphological changes in dendritic spines associated with long-term synaptic plasticity. Annu Rev Neurosci 24: 1071–1089.
Zhou Q, Homma KJ, Poo MM (2004) Shrinkage of dendritic spines associated with long-term depression of hippocampal synapses. Neuron 44:749–757.
Zola SM, Squire LR, Teng E, Stefanacci L, Buffalo EA, Clark RE (2000) Impaired recognition memory in monkeys after damage limited to the hippocampal region. J Neurosci 20:451–463.